Insulin-like Growth Factor 1 Promotes the Extension of Tracheal Epithelium in an *in Vitro* Tracheal Organ Culture Model

Ippei Kishimoto, MD[1], Hiroe Ohnishi, PhD[1], Kohei Yamahara, MD, PhD[2], Takayuki Nakagawa, MD, PhD[1], Masaru Yamashita, MD, PhD[3], Koichi Omori, MD, PhD[1], Norio Yamamoto, MD, PhD[1]*

[1]Department of Otolaryngology, Head and Neck Surgery, Graduate School of Medicine, Kyoto University, 54 Shogoin Kawahara-cho, Sakyo-ku, Kyoto, 606-8507, Japan

[2]Department of Otolaryngology - Head and Neck Surgery, Shizuoka City Hospital, 10-93 Ohte-machi, Aoi-ku, Shizuoka, 420-8630, Japan

[3]Department of Otolaryngology - Head and Neck Surgery, Kagoshima University Graduate School of Medical and Dental Sciences, 8-35-1 Sakuragaoka, Kagoshima, 420-8527, Japan

*Correspondence

Norio Yamamoto, MD, PhD

yamamoto@ent.kuhp.kyoto-u.ac.jp

Insulin-like Growth Factor 1 Promotes the Extension of Tracheal Epithelium in an *in Vitro* Tracheal Organ Culture Model

Abstract

OBJECTIVE: Rapid epithelialization is crucial to maintain tracheal patency and prevent potential graft failure in tracheal reconstruction after tracheal resection for cancer with tracheal infiltration or tracheal stenosis. Insulin-like growth factor 1 is a liver-secreted endocrine molecule that controls cell proliferation, differentiation, and apoptosis and has been reported to promote epithelialization in several organs. Here, we utilized mouse tracheal organ cultures to examine the effect of insulin-like growth factor 1 on tracheal epithelialization.

METHODS: The trachea was resected from thirteen-week-old female ICR mice, and cut into small plate-shaped tracheal sections. First, the expression of insulin-like growth factor 1 receptor was assessed by immunohistochemistry. Secondly, the tracheal sections were cultured for seven days in the culture medium, and the morphological change during the seven-day culture was assessed by immunohistochemistry, hematoxylin and eosin staining, and scanning electron microscopy. Moreover, the tracheal sections were cultured for 48 hours with different concentration of insulin-like growth factor 1 (0, 0.1, 1 and 10 μg/mL) in the

culture medium, and the extension length of the tracheal epithelium during culture was measured in order to assess the effect of topical IGF1 on tracheal epithelialization.

RESULTS: Immunohistochemistry showed that insulin-like growth factor 1 receptor was expressed in tracheal epithelium. Immunohistochemistry, hematoxylin and eosin staining, and scanning electron microscopy showed that the tracheal organ cultures were stable for at least seven days without apparent morphological damage. The effect of insulin-like growth factor 1 on tracheal epithelialization was examined in plate-shaped tracheal sections cultured in medium supplemented with or without insulin-like growth factor 1 for 48 hours. We also found that the epithelial edge of plate-shaped tracheal sections extended further along the surface of the tracheal section in culture medium containing insulin-like growth factor 1 compared with that in culture medium without insulin-like growth factor 1.

CONCLUSION: The current study using an *in vitro* mouse tracheal organ culture model demonstrated that topical insulin-like growth factor 1 treatment promoted the extension of tracheal epithelium, suggesting the potential utility of insulin-like growth factor 1 in aiding rapid tracheal epithelialization in patients requiring tracheal reconstruction using tissue-engineered tracheas.

Key words:

insulin-like growth factor-1; organ culture; re-epithelialization; regeneration; trachea

Introduction

Trachea is a tubular organ that has a U-shaped structure comprising hyaline cartilage in the anterior and lateral walls, with important functions related to respiration and vocalization. Total or partial tracheal resection is often necessary in cases of thyroid or laryngeal cancer with tracheal infiltration or stenosis and of tracheal cancer. In such cases, direct anastomosis after resection can be an appropriate procedure if the size of the resected tracheal section is small; however, high mechanical tension at the site of anastomosis can lead to severe and fatal postoperative complications such as anastomotic dehiscence (1). Thus, airway reconstruction is necessary if the resected tracheal length is >6 cm (2) or longer than half of the tracheal length in adults or one-third of the tracheal length in children (3, 4).

During the reconstruction of tubular organs including the trachea, epithelialization is crucial to maintain organ patency because the lack of an epithelial cell layer can lead to the over-proliferation of the underlying fibroblast layer and can result in stricture formation, stenosis, and potential graft failure (5). In addition, the tracheal epithelium plays an important role in mucus clearance and infection prevention (6, 7). In fact, the formation of the respiratory epithelium is considered a key component of therapies such as those using tissue-engineered tracheas (TETs) (2). The key components in TET are reproducible cell lines with the potential for generating respiratory epithelium and a scaffold for the reproduction of the

structural frame (8). Several clinical studies using TETs since 2004 showed promising results for the repair of long-segment tracheal defects (9). However, clinical studies reported that approximately two months were needed for the epithelialization of the transplanted TETs (10, 11). Thus, rapid epithelialization should be aimed for prompt stabilization of the graft and prevention of postoperative complications such as infection and stenosis.

Insulin-like growth factor 1 (IGF1) is a liver-secreted endocrine molecule that controls cell proliferation, differentiation, and apoptosis through paracrine and autocrine mechanisms (12, 13). We previously showed that local IGF1 applications using hydrogel protected cochlear hair cells from noise trauma in rats (14) and ischemic injury in gerbils (15). We also reported that IGF1 inhibited hair cell apoptosis and promoted cell cycle of supporting cells in the cochlea after pharmacological hair cell injury in mice (16). Based on these results, we conducted clinical trials of topical IGF1 therapy for idiopathic sudden sensorineural hearing loss in humans to demonstrate its efficacy and safety (17). Importantly, IGF1 was reported to promote epithelialization in several organs. For example, IGF1 exerted mitogenic and motogenic effects on keratinocytes *in vitro* and *in vivo* (18) and promoted gastric re-epithelialization and proliferation *in vitro* (19). Furthermore, IGF1 was reported to induce cell proliferation in primary cultures of canine and murine tracheal epithelial cells via a mitogenic response mediated by IGF1 receptors (20, 21). However, no studies to date have shown that IGF1 affected tracheal epithelial cells in tissue or organ cultures. The tracheal organ culture (TOC) system has been commonly used to study the host–pathogen interactions (22, 23). In

the TOC system, the respiratory epithelium is reported to remain viable for at least 120 hours, as assessed by ciliary movement and tissue morphology (24). In addition, TOC has the advantage over cell culture in that it mimics the natural state more closely and can be used for *in vitro* investigation of morphological and functional alterations in the respiratory epithelium (24).

Our goal is to promote tracheal epithelialization in transplanted TETs in clinical cases. In this study, in order to explore the future possibility of using IGF1 as a clinically applicable drug promoting tracheal epithelialization, we assessed the effect of IGF1 on epithelialization of the trachea using mouse TOCs.

Materials and Methods

Animals

Thirteen-week-old female ICR mice were purchased from SLC Japan (Hamamatsu, Japan). All animal procedures were approved by the Animal Research Committee of the Graduate School of Medicine at ***** University (****** 16080-3).

Tracheal resection and explant preparation

Immediately after the mice were euthanized using 100% carbon dioxide, the skin on the anterior neck of mice was incised and the trachea was immediately resected from the level of the cricoid to the carina (Figure 1a). The resected trachea was dissected in a plane perpendicular to the long axis of the trachea at a thickness of approximately two tracheal rings to obtain several ring-shaped tracheas (Figure 1b). Next, the membranous portion was removed from the ring-shaped trachea (Figure 1b, dashed lines), and the remaining cartilaginous section was cut into quarters in a plane parallel to the long axis of the trachea (Figure 1b, solid lines). The final plate-shaped tracheal section is shown in Figure 1c.

Tracheal organ cultures

TOCs were prepared with modifications to a previously reported protocol (25). Briefly, the mouse tracheal explants were washed three times in Hank's balanced salt solution containing 100 U/ml penicillin and 100 µg/mL streptomycin (Wako, Osaka, Japan) and cultured in Dulbecco's modified eagle's medium/F-12 (Nacalai Tesque, Kyoto, Japan) supplemented with 1% glutamax (Invitrogen, Carlsbad, CA, USA), 100 U/ml penicillin, and 100 µg/mL streptomycin (Wako) at 37°C in a humidified 5% CO_2 atmosphere. One to four tracheal sections (Figure 1c) were cultured in 300 µl of the culture medium described above in each well of a 24-well culture plate (Product Number: 3820-024, AGC TECHNO GLASS, Shizuoka, Japan). The culture medium was changed daily.

IGF1 treatment

To examine whether IGF1 affected growth of the tracheal epithelial cells, after 24 hours of preculture, plate-shaped tracheal sections (Figure 1c) were divided into four groups and different concentrations of IGF1 (0 [control], 0.1, 1, and 10 μg/mL; Orphan-Pacific Pharma, Tokyo, Japan) was administered in culture medium (Figure 2). There were six mice in each group. The culture medium was exchanged daily. After 48 hours of treatment with different concentrations of IGF1, the explants were examined by immunohistochemistry as described below to assess the effect of IGF1 on tracheal epithelialization. For the quantification of the IGF1 effects other than the extension length of the epithelia, we collected data from samples treated with 1 μg/mL of IGF1.

Immunohistochemistry and hematoxylin and eosin staining

The tracheal explants were fixed with 4% paraformaldehyde at 4°C for one hour, immersed in 30% sucrose in 0.1 M phosphate-buffered saline overnight, embedded in optimal cutting temperature compound (Sakura Finetek USA, Torrance, CA, USA), sectioned at 10-μm , and mounted on adhesive glass slides (MAS-01 15; Matsunami Glass, Osaka, Japan). For immunohistochemistry, the specimens were incubated with the following primary antibodies at 4°C overnight: mouse monoclonal anti-acetylated Tubulin (1:500, Catalog # T7451,

Sigma-Aldrich, St. Louis, MO, USA), rabbit anti-IGF-1 receptor β (1:100, Catalog # 3027S, Cell Signaling Technology, Danvers, MA, USA) with or without IGF-1 Receptor β blocking peptide (1:50, Catalog # 1525, Cell Signaling Technology), rat anti-mouse E-cadherin (1:1000, Code # M108, TaKaRa Bio USA, Mountain View, CA, USA), or rabbit monoclonal anti-Ki-67 (1:500, Catalog # MA5-14520, Invitrogen). For evaluating the reactive specificity of rabbit anti-IGF-1 receptor β antibody, IGF-1 Receptor β blocking peptide (1:50, Catalog # 1525, Cell Signaling Technology) or phosphate-buffered saline (PBS) was mixed with the primary antibody solution containing rabbit anti-IGF-1 receptor β antibody and incubated for 1 hour at room temperature before incubation with specimens. The specimens were subsequently incubated with the following secondary antibodies for one hour at room temperature: Alexa 568-conjugated anti-mouse IgG (Life Technologies, Carlsbad, CA), Alexa 488- or 594-conjugated anti-rabbit IgG (Life Technologies), or Alexa 488- or 568-conjugated anti-rat IgG (Life Technologies) antibodies. Cell nuclei and actin filaments were counterstained with 4',6-diamidino-2-phenylindole dihydrochloride (DAPI; Invitrogen) and Alexa 633-labeled phalloidin (Catalog # A22284, Invitrogen), respectively. Fluorescent images were acquired with a Leica TCS SPE microscope (Leica Microsystems, Wetzlar, Germany). For hematoxylin and eosin (H&E) staining, the specimens were stained with Mayer's hematoxylin solution (Wako) and Eosin Alcohol Solution, acid extract (Wako). Images were captured using an Olympus DP70 digital camera (Olympus, Tokyo, Japan) on an Olympus BX50 microscope (Olympus).

Measurement of tracheal epithelial extension

Tracheal epithelial extension length was determined in the immunofluorescent images by E-cadherin staining acquired with a Leica TCS SPE microscope with a 10x objective lens (Leica Microsystems) in the middle section of a plate-shaped tracheal section (Figure 1c, dashed line). We measured the tracheal epithelial extension from the edge of the tracheal cartilage prepared before culture. The starting points of the measurement were identified in images (Figures 1d and 6c) as the point on the luminal surface of the epithelium crossed by the straight line (dotted lines in Figures 1d and 6c). This line is perpendicular to the adventitial surface line (dashed lines in Figures 1d and 6c) of the tracheal cartilage and attaches to the cartilage edge. We used ImageJ (National Institutes of Health, Bethesda, MD, USA) for the measurement (Figures 1d and 6c, x or y). The sum of the measures on both sides (Figure 1d and 6c, x + y) was defined as the extension length of the tracheal epithelium. The data from one mouse were the averaged extension lengths from one to four plate-shaped tracheal sections from the mouse.

Definition of the cell proliferation ratio in extended tracheal epithelium

The cross-sectional area of the extended tracheal epithelium was defined as the E-cadherin-immunostained area from the original edge of the epithelium to the edge of the extended

epithelium, as described above. The cell proliferation ratio in extended tracheal epithelium was defined as the ratio of the number of Ki67-positive cells to the number of DAPI-positive cells in extended tracheal epithelium.

Definitions of average width, thickness, and cross-sectional area of cells in the extended tracheal epithelium during explant culture

In an image acquired with a Leica TCS SPE microscope with a 20x objective lens (Leica Microsystems). The area of extended tracheal epithelium was enclosed with a polygonal line and measured by using area measurement function of ImageJ. A scheme of the average width and thickness, and the average area of an epithleial cell is shown in Figure 1e.

1. The average width of an epithelial cell in the extended tracheal epithelium was calculated by dividing the cross-sectional area of the extended tracheal epithelium by the number of DAPI-positive cells in the extended tracheal epithelium.
2. The average thickness of the extended epithelium was calculated by dividing the cross-sectional area of the extended tracheal epithelium by the extension length of the tracheal epithelium.
3. The average area of an epithelial cell in the extended tracheal epithelium was calculated by dividing the cross-sectional area of the extended tracheal epithelium by the number of DAPI-positive cells in the extended tracheal epithelium.

Scanning electron microscopy

Tracheal tissue before and after seven days in organ cultures was observed by scanning electron microscopy to examine the morphology of cilia. Briefly, the tissues were fixed with 4% paraformaldehyde containing 2% glutaraldehyde in phosphate buffer at 4°C overnight. Next, the samples were dehydrated, dried by the critical-point drying method, and coated with a thin layer of platinum-palladium. The specimens were examined using a scanning electron microscope (S-4700; Hitachi, Tokyo, Japan).

Statistical analysis

Comparison of the extension length of the tracheal epithelium among the four groups was analyzed using the single-factor ANOVA followed by Holm–Sidak's multiple comparisons test. Comparison of cell proliferation and cell morphology of extended tracheal epithelium during organ culture between control samples and samples with 1 μg/mL of IGF1 was performed by the paired *t*-test. Differences with a $p < 0.05$ were considered statistically significant. All numerical data were presented with mean ± standard error of the mean.

Results

IGF1 receptor is expressed in the tracheal epithelium of mouse tracheal organ cultures

The IGF1 receptor was reported to be expressed in the respiratory epithelium (26). In order to confirm the expression of the IGF1 receptor in the tracheal epithelium of mice, we first examined the IGF1 receptor expression levels in tracheal epithelium by immunohistochemistry (n = 4). We observed IGF1 receptor immunoreactivity in all types of cells of the tracheal epithelium, as indicated by E-cadherin immunostaining, including ciliated, secretory, and basal cells, in four different mice (Figure 3a-d). The immunoreactive signal of the IGF1 receptor was remarkably decreased when we added the blocking peptide in the primary antibody solution (Figure 3e-h), indicating the signal was specific to the IGF1 receptor. The findings suggested that all types of tracheal epithelial cells expressed the IGF1 receptor.

The morphology of the mouse tracheal organ cultures are preserved for seven days

We next determined whether TOCs were stable over a number of days by comparison of the histological features of the plate-shaped tracheal sections (Figure 1b) before and seven days after the initiation of organ culture (Figures 2 and 4). We found that the layered structure of the sections, including the epithelium, basal membrane, and tracheal cartilage, determined by H&E staining (a and a’ in Figure 4), was preserved at both time points in four different mice. In addition, the intercellular junctions between the tracheal epithelial cells were also

maintained throughout the seven days, as shown by E-cadherin immunostaining (b and b' in Figure 4). Acetylated tubulin immunostaining (c and c' in Figure 4) and scanning electron microscopy (d and d' in Figure 4) revealed that the morphology of the cilia was retained at seven days after the initiation of organ culture in four different mice. These findings suggested that the mouse TOCs were stable for at least seven days with no apparent morphological damage.

The tracheal epithelium extends along the surface of the mouse tracheal organ cultures

Next, we evaluated the growth of tracheal epithelium in mouse TOCs by assessing the epithelium of the plate-shaped tracheal sections before (Figure 5) and seven days after the initiation of organ culture (Figure 6a and 6b) by immunohistochemistry and H&E staining. The tracheal epithelium was observed on the mucosal side of the explant before culture as determined by the E-cadherin staining (Figure 5). In contrast, the tracheal epithelium was present on the adventitial side of the explant as well as on the mucosal side after 7-day organ culture (arrowheads in Figure 6a and 6b). Similar results were found in four different mice. These findings suggested that the edge of the tracheal epithelium extended along the surface of the plate-shaped tracheal sections and surrounded the tracheal cartilage during the seven days of culturing.

IGF1 induces tracheal epithelial growth in mouse tracheal organ cultures

We next determined the effect of topical IGF1 on the growth of tracheal epithelium in our mouse TOCs using six mice. After 48 hours following treatment with or without IGF1, the length of tracheal epithelial extension (x + y in Figure 1d and 6c) was significantly higher in the plate-shaped tracheal sections treated with 0.1, 1, and 10 μg/mL of IGF1 compared with the control sections (p = 0.0329, 0.0028, and 0.0329, respectively) (Figure 6d). Overall, these results suggested that IGF1 was effective in tracheal epithelial growth in mouse TOCs.

IGF1 effect on cell proliferation and cell morphology of the tracheal epithelium

To elucidate the mechanism by which topical administration of IGF1 promotes tracheal epithelium extension in our explant culture model, we next examined cell proliferation in the extended tracheal epithelium. We found that the cell proliferation ratio in extended tracheal epithelium was 27.5 ± 6.7% and 15.5 ± 3.7% (n = 4 each) in control and experimental samples, respectively (Figure 7a). Statistical analysis found no significant differences between the two groups (paired t-test, p = 0.13).

Next we examined whether topical administration of IGF1 promoted the increase in epithelial cell numbers during explant culture. The cell number in extended tracheal epithelium in one tracheal piece were 42.3 ± 7.0 and 59.0 ± 13.0 (n = 4 each) in control and experimental

samples, respectively) (Figure 7b). Statistical analysis found no significant differences between the two groups (paired *t*-test, $p = 0.19$).

Lastly, to assess the effect of IGF1 on the morphology of each epithelial cell during epithelium extension, we calculated the average width, thickness, and cross-sectional area of cells in the extended tracheal epithelium. The average width, thickness, and cross-sectional area of an epithelial cell along the surface of the control and experimental tracheal sections were 12.2 ± 1.0 and 14.6 ± 1.3 µm, 7.7 ± 1.2 and 8.0 ± 0.3 µm, and 94.2 ± 9.2 and 115.1 ± 8.0 μm^2 ($n = 4$ each), respectively (Figure 7c−e). There were no significant differences in width, thickness, and cross-sectional area between control and experimental samples with 1 µg/mL of IGF1 (paired *t*-test, $p = 0.23$, 0.78, and 0.27, respectively).

Discussion

In the present study, we determined whether IGF1 induced tracheal epithelialization by assessing the extension of the epithelial edge to surround the tracheal cartilage surface of plate-shaped tracheal sections in an *in vitro* mouse TOC model. In this first report investigating IGF1-mediated epithelialization of the trachea in an organ culture model, we demonstrated that treatment with 0.1, 1 and 10 µg/mL of IGF1 promoted the epithelial extension.

Injury model of tracheal epithelialization

To evaluate the rate of tracheal epithelialization, we cultured plate-shaped tracheal sections for 48 hours prior to evaluating epithelial extension from the cutting edge of the tracheal section. An advantage of this approach is the ability to evaluate the effect of IGF1 on tracheal epithelialization in the absence of tracheal injury. Numerous studies investigating tracheal epithelialization utilized animal models of tracheal injury such as chemical injury by sodium hydroxide (25), hydrochloric acid (27), sulfur dioxide (28), or chlorine gas (29) and mechanical injury by a scalpel (25) or a steel wire brush (30). However, none of these methods are able to create a consistent or stable tracheal injury, which hinders replicating the same condition across different samples. The method we used in this study allowed maintenance of experimental conditions that were consistent across culture sections as the injury to the tracheal intraluminal surface was unnecessary. This method only requires the preparation uniformly sized tracheal sections with a micro-scalpel or scissors from the adult mouse trachea. Additionally, the quantification of the rate of tracheal epithelialization is simple because only the length of the tracheal epithelium extending from the cutting edge was measured. This approach can be applied to experiments to examine the effect of different drugs or growth factors other than IGF1 on the extension of the tracheal epithelium.

Effect of IGF1 on the tracheal epithelium through the IGF1 receptor

It has been reported that activation of the IGF1 receptor by IGF1 is implicated in cell survival, growth, differentiation, and migration in epithelial and mesenchymal tissues (19, 31, 32). As the IGF1 receptor is reported to be expressed in the respiratory epithelium (26), we first confirmed the expression of the IGF1 receptor in every cell type of the tracheal epithelium. In this study, topical administration of IGF1 promoted tracheal epithelium extension from the cutting edge of the tracheal section during organ culture, which we think was mediated by binding between IGF1 and the IGF1 receptor. Although the previous study (26) showing the expression of IGF1 receptor in the respiratory epithelium demonstrated that IGF1 receptor was related to carcinogenesis due to smoking, it didn't show that IGF1 affected on the extension of the respiratory epithelium. Thus, the novelty of our study is that we first revealed that IGF1 promotes the tracheal epithelium extension. Our analysis of the cellular morphology of the extended tracheal epithelium did not clearly reveal the underlying mechanism of this effect of IGF1; neither cell number nor cell width was shown to significantly contribute to the promotion of tracheal epithelium extension. Topical administration of IGF1 was reported to induce cell migration and proliferation *in vitro* in a study using a rat gastric mucosal epithelial cell line (19) and to increase the olfactory epithelium proliferation an *in vivo* mouse model (33). In our present study, on the other hand, the ratio of Ki67-positive cells in the extended tracheal epithelium in IGF1-treated samples was not higher than that in control samples; rather, it tended mildly to be lower in the IGF1 group than in the control group, which may suggest that topical administration of IGF1

suppresses proliferation of the tracheal epithelium in organ culture. The re-epithelialization of the tracheal epithelium after mechanical injury has several steps (34). The first step is spreading and migration of basal cells without cell proliferation, followed by a repair process with cell proliferation. The process of tracheal epithelium extension in our culture model includes the spreading and migration of epithelial cells both with and without cell proliferation. Therefore, the promotion of tracheal epithelium extension by topical administration of IGF1 in the present study may have been induced not through increased proliferation of epithelial cells, but through other mechanisms, such as spreading of epithelial cells. That is, our results may suggest that in our experimental model IGF1 doesn't promote proliferation of epithelial cells, which was reported in the previous *in vitro* study (20, 21), but rather promotes spreading and migration of tracheal epithelial cells without cell proliferation.

Difference between natural injury and our *in vitro* model

The results of the current study should be interpreted carefully. The trajectory of the tracheal epithelium extending from the cutting edge in this study may not be identical to that occurring during the regeneration of injured tracheal epithelium *in vivo.* During tracheal wound healing, if the wound is superficial and does not reach the basal membrane, the surface epithelium can regenerate through proliferation and differentiation of basal cells that have a high proliferative capacity (35). If the tissue injury is severe and involves both the epithelial cells and the submucosal layer, healing requires the deposition of collagen as well

as regeneration, leading to scar formation (35). In this study, in order to evaluate epithelialization, we created a sharp cutting edge from the epithelial layer through the tracheal cartilage. However, such injury may be different from natural injuries, including superficial epithelial wounding or damage to both epithelial cells and the submucosal layer. Furthermore, epithelialization from the cutting edge to the backside of the tracheal lumen during culture may be different from the physiological re-epithelialization of injured tracheal epithelium *in vivo*. Therefore, the current results may not directly demonstrate the IGF1-mediated promotion of epithelialization which could be utilized in clinical use. In order to confirm clinical effects of IGF1 on injured tracheal epithelium, it is necessary in the future to assess the IGF1 effect on re-epithelialization of tracheal lumen using its injury model. Our findings in mouse TOCs, however, clearly demonstrated that IGF1 led to a significantly more efficient tracheal epithelial extension compared to the control treatment. Thus, our easy-to-prepare *in vitro* experimental model is useful for screening drugs or growth factors that might be capable of regenerating the tracheal epithelium.

Topical administration of IGF1 for tracheal epithelialization in clinical use

Many strategies other than drug treatment were reported for tracheal epithelialization in TETs. Such approach includes the modification of tissue-engineered scaffolds with optimally concentrated collagen sponges (36, 37) or with collagen vitrigel (38, 39). Another technique is the use of specific cells including fibroblasts (39, 40) and adipose-derived stem cells (41)

in combination with the scaffolds. In addition, Tani *et al.* examined the effect of basic fibroblast growth factor (bFGF) in tracheal epithelialization in a rat model (42). The authors laid collagen vitrigel-sponge scaffolds containing bFGF onto tracheal defects in rats and showed that bFGF promoted epithelial regeneration of the scaffold. They showed the regenerative effect of bFGF quantitatively based on the percentage of ciliated cells among regenerative epithelial cells and the extent of neovascularization in the regenerative subepithelial layer. Combination of these strategies with IGF1 treatment might further enhance the regeneration of tracheal epithelium.

Conclusion

The current study using an *in vitro* mouse TOC model demonstrated that topical IGF1 treatment promoted the extension of tracheal epithelium. The result suggested the potential utility of IGF1 in aiding rapid tracheal epithelialization in patients requiring tracheal reconstruction using TETs. In addition, the *in vitro* experimental system used in the current study is an easy-to-implement and useful method for screening drugs or substances that can promote epithelialization of the trachea.

Author contributions

IK, HO, KY, TN, KO, and NY designed and conceived the experiments. IK, KY, and HO performed the experiments. IK and KY acquired confocal images. IK analyzed the data. IK, HO, MY, and NY wrote the manuscript. KO and MY obtained funding.

Acknowledgments

We are grateful to Keiko Okamoto-Furuta and Haruyasu Kohda from the Division of Electron Microscopic Study, Center for Anatomical Studies, Graduate School of Medicine, Kyoto University for the technical support in electron microscopy.

Funding

This study was financially supported by JSPS KAKENHI Grant Number JP******** and by Otolaryngology Research Fund ***** University.

Disclosure Statement

The authors declare that there is no conflict of interest.

References

1. Rotolo N, Cattoni M, Imperatori A. Complications from tracheal resection for thyroid carcinoma. Gland Surg. 2017;6(5):574-8.
2. Law JX, Liau LL, Aminuddin BS, Ruszymah BH. Tissue-engineered trachea: A review. Int J Pediatr Otorhinolaryngol. 2016;91:55-63.
3. Grillo HC. Tracheal replacement: a critical review. Ann Thorac Surg. 2002;73(6):1995-2004.
4. Kucera KA, Doss AE, Dunn SS, Clemson LA, Zwischenberger JB. Tracheal replacements: part 1. ASAIO J. 2007;53(4):497-505.
5. Saksena R, Gao C, Wicox M, de Mel A. Tubular organ epithelialisation. J Tissue Eng. 2016;7:2041731416683950.
6. Satir P, Christensen ST. Overview of structure and function of mammalian cilia. Annu Rev Physiol. 2007;69:377-400.
7. Stannard W, O'Callaghan C. Ciliary function and the role of cilia in clearance. J Aerosol Med. 2006;19(1):110-5.
8. Doss AE, Dunn SS, Kucera KA, Clemson LA, Zwischenberger JB. Tracheal replacements: Part 2. ASAIO J. 2007;53(5):631-9.
9. Abouarab AA, Elsayed HH, Elkhayat H, Mostafa A, Cleveland DC, Nori AE. Current Solutions for Long-Segment Tracheal Reconstruction. Ann Thorac Cardiovasc Surg. 2017;23(2):66-75.
10. Jungebluth P, Alici E, Baiguera S, Blomberg P, Bozóky B, Crowley C, et al. Tracheobronchial transplantation with a stem-cell-seeded bioartificial nanocomposite: a proof-of-concept study. Lancet. 2011;378(9808):1997-2004.
11. Omori K, Nakamura T, Kanemaru S, Asato R, Yamashita M, Tanaka S, et al. Regenerative medicine of the trachea: the first human case. Ann Otol Rhinol Laryngol. 2005;114(6):429-33.
12. Jenkins PJ, Bustin SA. Evidence for a link between IGF-I and cancer. Eur J Endocrinol. 2004;151 Suppl 1:S17-22.
13. Varela-Nieto I, Hartl M, Gorospe I, León Y. Anti-apoptotic actions of insulin-like growth factors: lessons from development and implications in neoplastic cell transformation. Curr Pharm Des. 2007;13(7):687-703.
14. Iwai K, Nakagawa T, Endo T, Matsuoka Y, Kita T, Kim TS, et al. Cochlear protection by local insulin-like growth factor-1 application using biodegradable hydrogel. Laryngoscope. 2006;116(4):529-33.
15. Fujiwara T, Hato N, Nakagawa T, Tabata Y, Yoshida T, Komobuchi H, et al. Insulin-like growth factor 1 treatment via hydrogels rescues cochlear hair cells from ischemic injury. Neuroreport. 2008;19(16):1585-8.
16. Hayashi Y, Yamamoto N, Nakagawa T, Ito J. Insulin-like growth factor 1 inhibits hair cell apoptosis and promotes the cell cycle of supporting cells by activating different downstream cascades after pharmacological hair cell injury in neonatal mice. Mol Cell Neurosci. 2013;56:29-38.
17. Nakagawa T, Sakamoto T, Hiraumi H, Kikkawa YS, Yamamoto N, Hamaguchi K, et al. Topical insulin-like growth factor 1 treatment using gelatin hydrogels for glucocorticoid-resistant sudden sensorineural hearing loss: a prospective clinical trial. BMC Med. 2010;8:76.
18. Seeger MA, Paller AS. The Roles of Growth Factors in Keratinocyte Migration. Adv Wound Care (New Rochelle). 2015;4(4):213-24.
19. Nguyen T, Chai J, Li A, Akahoshi T, Tanigawa T, Tarnawski AS. Novel roles of local insulin-like growth factor-1 activation in gastric ulcer healing: promotes actin polymerization, cell proliferation, re-epithelialization, and induces cyclooxygenase-2 in a phosphatidylinositol 3-kinase-dependent manner. Am J Pathol. 2007;170(4):1219-28.
20. Retsch-Bogart GZ, Stiles AD, Moats-Staats BM, Van Scott MR, Boucher RC, D'Ercole AJ. Canine tracheal epithelial cells express the type 1 insulin-like growth factor receptor and proliferate in response to insulin-like growth factor I. Am J Respir Cell Mol Biol. 1990;3(3):227-34.

21. Kumar RK, Maronese SE, O'Grady R. Serum-free culture of mouse tracheal epithelial cells. Exp Lung Res. 1997;23(5):427-40.
22. Schmidt RC, Maassab HF, Davenport FM. Infection by influenza A viruses of tracheal organ cultures derived from homologous and heterologous hosts. J Infect Dis. 1974;129(1):28-36.
23. Reemers SS, Groot Koerkamp MJ, Holstege FC, van Eden W, Vervelde L. Cellular host transcriptional responses to influenza A virus in chicken tracheal organ cultures differ from responses in in vivo infected trachea. Vet Immunol Immunopathol. 2009;132(2-4):91-100.
24. Leeming G, Meli ML, Cripps P, Vaughan-Thomas A, Lutz H, Gaskell R, et al. Tracheal organ cultures as a useful tool to study Felid herpesvirus 1 infection in respiratory epithelium. J Virol Methods. 2006;138(1-2):191-5.
25. Hicks WL. Increased expression of keratinocyte growth factor represents a stereotypic response to tracheal lumenal insult independent of injury mechanism. Laryngoscope. 1999;109(10):1552-9.
26. Kim WY, Jin Q, Oh SH, Kim ES, Yang YJ, Lee DH, et al. Elevated epithelial insulin-like growth factor expression is a risk factor for lung cancer development. Cancer Res. 2009;69(18):7439-48.
27. Ramphal R, Pyle M. Adherence of mucoid and nonmucoid Pseudomonas aeruginosa to acid-injured tracheal epithelium. Infect Immun. 1983;41(1):345-51.
28. Ishibashi Y, Okamura T, Masumoto Y, Tachiiri T, Momo K. [Effects of carbocisteine on airway inflammation and related events in SO2-exposed rats]. Nihon Kokyuki Gakkai Zasshi. 2001;39(1):17-23.
29. O'Koren EG, Hogan BL, Gunn MD. Loss of basal cells precedes bronchiolitis obliterans-like pathological changes in a murine model of chlorine gas inhalation. Am J Respir Cell Mol Biol. 2013;49(5):788-97.
30. Hillel AT, Namba D, Ding D, Pandian V, Elisseeff JH, Horton MR. An in situ, in vivo murine model for the study of laryngotracheal stenosis. JAMA Otolaryngol Head Neck Surg. 2014;140(10):961-6.
31. LeRoith D, Werner H, Beitner-Johnson D, Roberts CT, Jr. Molecular and cellular aspects of the insulin-like growth factor I receptor. Endocr Rev. 1995;16(2):143-63.
32. Rabinovsky ED. The multifunctional role of IGF-1 in peripheral nerve regeneration. Neurol Res. 2004;26(2):204-10.
33. Ueha R, Kondo K, Ueha S, Yamasoba T. Dose-Dependent Effects of Insulin-Like Growth Factor 1 in the Aged Olfactory Epithelium. Front Aging Neurosci. 2018;10:385.
34. Coraux C, Hajj R, Lesimple P, Puchelle E. [Repair and regeneration of the airway epithelium]. Med Sci (Paris). 2005;21(12):1063-9.
35. Delaere P, Van Raemdonck D. Tracheal replacement. J Thorac Dis. 2016;8(Suppl 2):S186-96.
36. Nakaegawa Y, Nakamura R, Tada Y, Nomoto Y, Imaizumi M, Suzuki R, et al. Effect of Structural Differences in Collagen Sponge Scaffolds on Tracheal Epithelium Regeneration. Ann Otol Rhinol Laryngol. 2016;125(2):115-22.
37. Suzuki R, Nakamura R, Nakaegawa Y, Nomoto Y, Fujimoto I, Semura K, et al. Optimal bovine collagen concentration to achieve tracheal epithelial coverage of collagen sponges. Laryngoscope. 2016;126(12):E396-E403.
38. Tada Y, Suzuki T, Takezawa T, Nomoto Y, Kobayashi K, Nakamura T, et al. Regeneration of tracheal epithelium utilizing a novel bipotential collagen scaffold. Ann Otol Rhinol Laryngol. 2008;117(5):359-65.
39. Nomoto Y, Kobayashi K, Tada Y, Wada I, Nakamura T, Omori K. Effect of fibroblasts on epithelial regeneration on the surface of a bioengineered trachea. Ann Otol Rhinol Laryngol. 2008;117(1):59-64.
40. Okano W, Nomoto Y, Wada I, Kobayashi K, Miyake M, Nakamura T, et al. Bioengineered trachea with fibroblasts in a rabbit model. Ann Otol Rhinol Laryngol. 2009;118(11):796-804.
41. Kobayashi K, Suzuki T, Nomoto Y, Tada Y, Miyake M, Hazama A, et al. A tissue-engineered trachea derived from a framed collagen scaffold, gingival fibroblasts and adipose-derived stem cells.

496 Biomaterials. 2010;31(18):4855-63.
497 42. Tani A, Tada Y, Takezawa T, Imaizumi M, Nomoto Y, Nakamura T, et al. Regeneration of
498 tracheal epithelium using a collagen vitrigel-sponge scaffold containing basic fibroblast growth factor.
499 Ann Otol Rhinol Laryngol. 2012;121(4):261-8.
500

501

Figure legends

Figure 1. Tracheal resection and organ culture preparation. (a) The trachea from the level of the cricoid to the carina was resected from mice (a yellow box). TC, thyroid cartilage; CC, cricoid cartilage. (b) The resected trachea was dissected into ring-shaped trachea sections with a thickness of approximately two tracheal rings. The membranous portion of the ring-shaped trachea was dissected, shown by two dashed lines. The cartilaginous portion of the trachea was cut at three solid lines, resulting in four sections. MP, membranous portion. (c) A plate-shaped tracheal section which was cut from the cartilaginous portion of the ring-shaped trachea. The dashed line indicates the midline of the section, which was used for evaluation of the growth of the tracheal epithelium in organ culture. (d) Scheme of a tracheal section in a cross-sectional view before and after explant culture. The two blue dots show original edges of the epithelium before culturing and the starting points to measure the extension of tracheal epithelia. These points are defined as the points on the luminal surface of the epithelium crossed by the straight line (dotted lines). This line is perpendicular to the adventitial surface line (dashed lines) of the tracheal cartilage and attaches to the cartilage edge. The sum of the extended length in both directions (x + y) is defined as the extension length of the tracheal epithelium. (e) Scheme of a green box area in Figure 1d. Images of the width, thickness, and cross-sectional area of a cell in the extended tracheal epithelium are shown. Scale bar, 1 mm (a and b) and 200 μm (c)

Figure 2. The schematic overview of tracheal organ culture. The plate-shaped tracheal sections (Figure 1c) were evaluated by H&E staining, IHC, and SEM before initiating the culture and after seven days without IGF1 treatment to show the quality of the cultured tracheal sections. To evaluate the effect of IGF1 on tracheal epithelial growth, the tracheal epithelial extension during organ culture was evaluated by H&E staining and IHC before starting the culture and after 48 hours of treatment with or without IGF1. H&E, hematoxylin and eosin; IGF1, insulin-like growth factor 1; IHC, immunohistochemistry; SEM, scanning electron microscope

Figure 3. Expression of the IGF1 receptor in tracheal epithelium. The IGF1 receptor expression in tracheal epithelia was examined by immunohistochemistry. The tracheal sections were co-stained with antibodies against IGF1 receptor (a, e), E-cadherin (for tracheal epithelium; b, f), and phalloidin (for actin filaments; c, g). Phosphate-buffered saline (PBS) (a−d) or IGF-1 Receptor β blocking peptide (e−h) was mixed with the primary antibody solution containing rabbit anti-IGF-1 receptor β antibody. The IGF1 receptor expression is detected in the tracheal epithelium, as shown in the merged image (d), but not detected when blocking peptide was administered (h). IGF1, insulin-like growth factor 1; TE, tracheal epithelium; SM, submucosa; TC, tracheal cartilage. Scale bar, 20 μm

Figure 4. Histological findings before and after tracheal organ culture. H&E staining images (a, a') are shown by cartilage cross-section view, and the surface of the tracheal lumen was captured by immunostaining (b, b', c, c') and SEM images (d, d'). (a), (b), (c) and (d) Images from the tissue before starting the culture. (a'), (b'), (c') and (d') Images from the tissue after 7-day organ cultures. The tissue structure of the trachea including the epithelium, basal membrane, and tracheal cartilage is shown by H&E staining (a, a'). E-cadherin immunostaining (b, b') shows that the epithelial layer is preserved. The acetylated tubulin immunostaining (c, c') and scanning electron microscopy (d, d') show that morphology of tracheal cilia is retained in 7-day organ cultures. Scale bar, 1 μm (d, d') and 10 μm (a, a', b, b', c, c'). H&E, hematoxylin and eosin

Figure 5. Evaluation of the epithelium of the plate-shaped tracheal sections before starting culture. The epithelial cell layer is indicated as the darkly stained area by H&E staining on the surface of the plate-shaped tracheal section (a, a'), and the intercellular space between epithelial cells is immunostained with the anti-E-cadherin antibody and counterstained with DAPI (b, b'). The white boxes in a and b are magnified in a' and b', respectively. H&E, hematoxylin and eosin; TE, tracheal epithelium; TC, tracheal cartilage. Scale bar, 100 μm (a, b) and 10 μm (a', b')

Figure 6. Evaluation of the epithelium of the plate-shaped tracheal section after seven days in organ culture, and extension of the epithelial cell layer in tracheal organ cultures treated with or without IGF1 for 48 hours. (a) (b) After seven days of organ culture, the epithelial cell layer, indicated by H&E staining (a) and E-cadherin immunostaining (b), is found on the entire surface of the plate-shaped tracheal section (arrowheads in a and b, b', and b"). The two white boxes in b are magnified in b' and b''. (c) After 48 hours of organ culture, the edge of the epithelial cell layer, indicated by E-cadherin staining, extends along the surface of the plate-shaped tracheal section. The extension length of the tracheal epithelium (x + y) is calculated in each tracheal section. (d) The tracheal epithelial growth is significantly better in organ cultures treated with 0.1, 1, or 10 µg/mL IGF1 compared with those not treated with IGF1 (control). The data are expressed as means ± standard error of the mean. $*p < 0.05$, $**p < 0.01$, single-factor ANOVA followed by Holm–Sidak's multiple comparisons test, analysis of variance; H&E, hematoxylin and eosin; IGF1, insulin-like growth factor 1; TE, tracheal epithelium; TC, tracheal cartilage. Scale bar, 100 µm (a, b), 10 µm (b', b''), and 100 µm (c)

Figure 7. Comparison of cell proliferation and cell morphology of the extended tracheal epithelium during organ culture between control and IGF1 treated samples. (a) Ratio of Ki67 positivity in DAPI-positive cells. (b) Number of epithelial cells that are positive for DAPI staining. (c) Average width of an epithelial cell in the extended tracheal epithelium. (d) Average thickness of the extended tracheal epithelium. (e) Average area of an epithelial cell

in the extended tracheal epithelium. The data are expressed as mean ± standard error of the mean. The numbers within bars show the numbers of mice in each sample group. Differences with $p < 0.05$ were considered statistically significant.

Figure 1

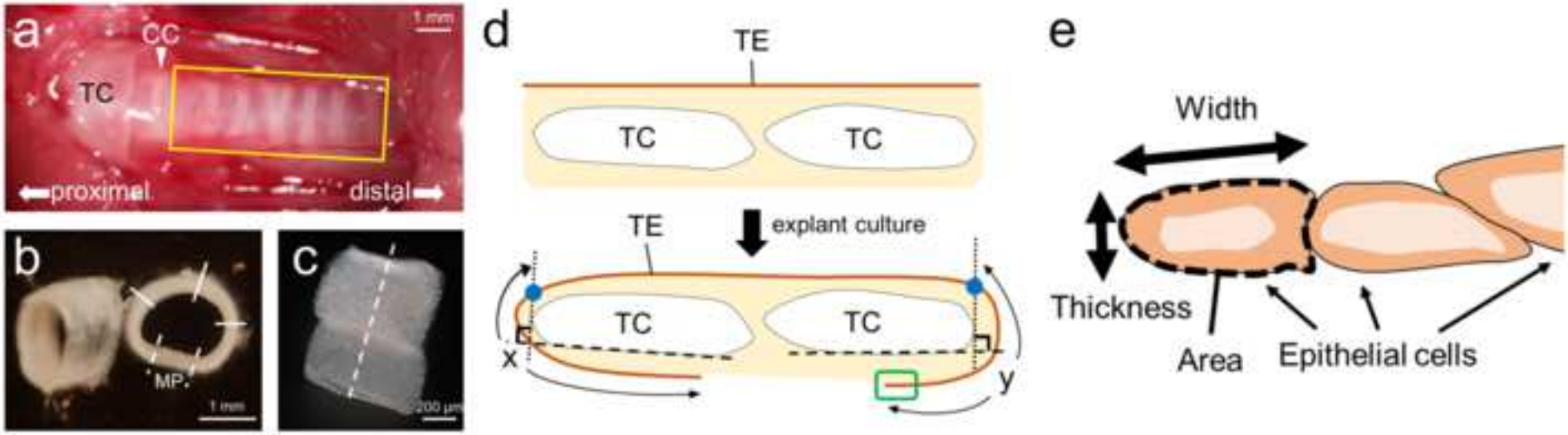
a
CC
TC
1 mm
proximal
distal
b
MP
1 mm
c
200 µm
d
TE
TC
TC
explant culture
TE
TC
TC
x
y
e
Width
Thickness
Area
Epithelial cells

Figure 2

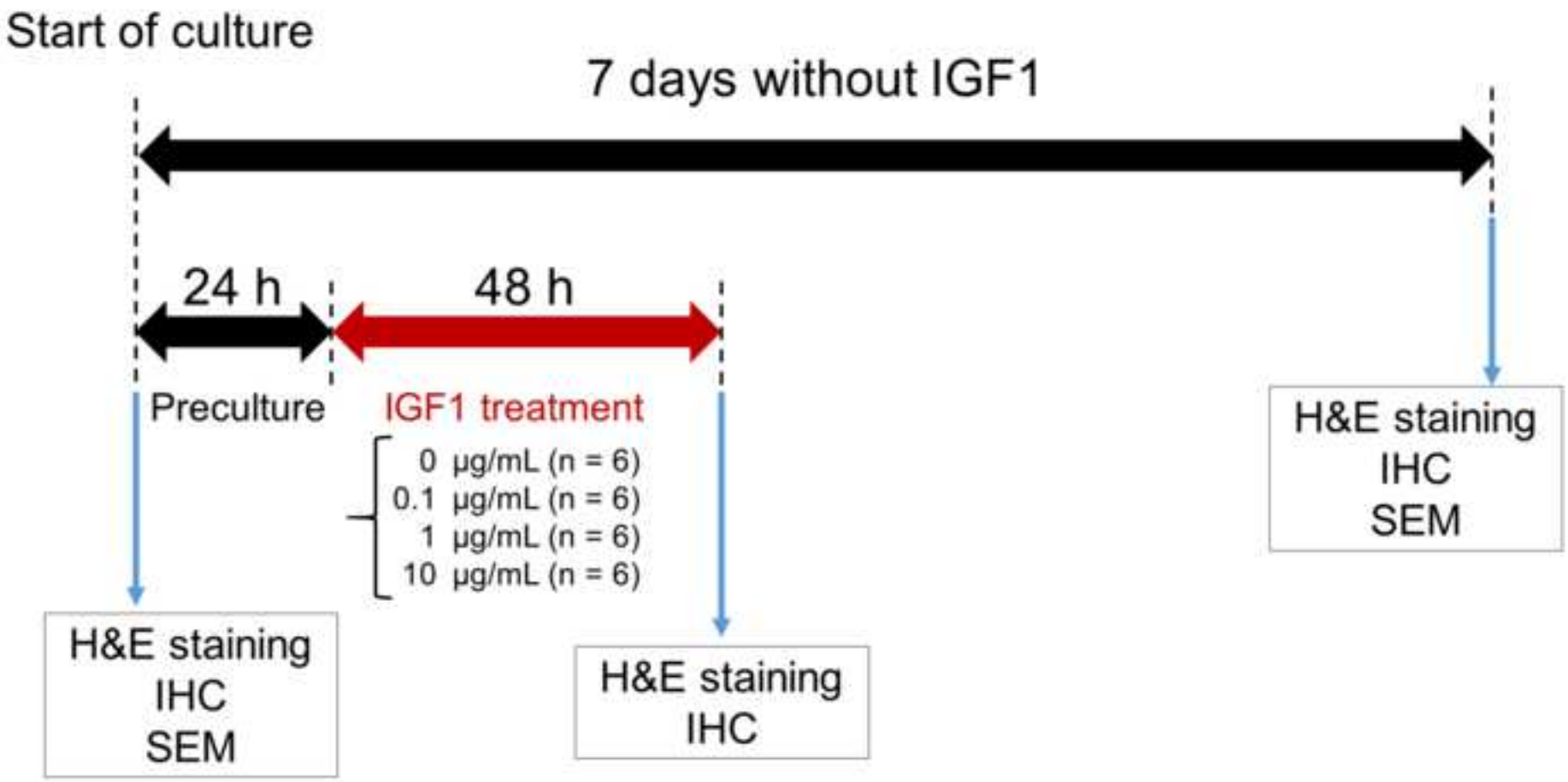
Start of culture
7 days without IGF1
24 h
48 h
Preculture
IGF1 treatment
0 µg/mL (n = 6)
0.1 µg/mL (n = 6)
1 µg/mL (n = 6)
10 µg/mL (n = 6)
H&E staining
IHC
SEM
H&E staining
IHC
H&E staining
IHC
SEM

Figure3

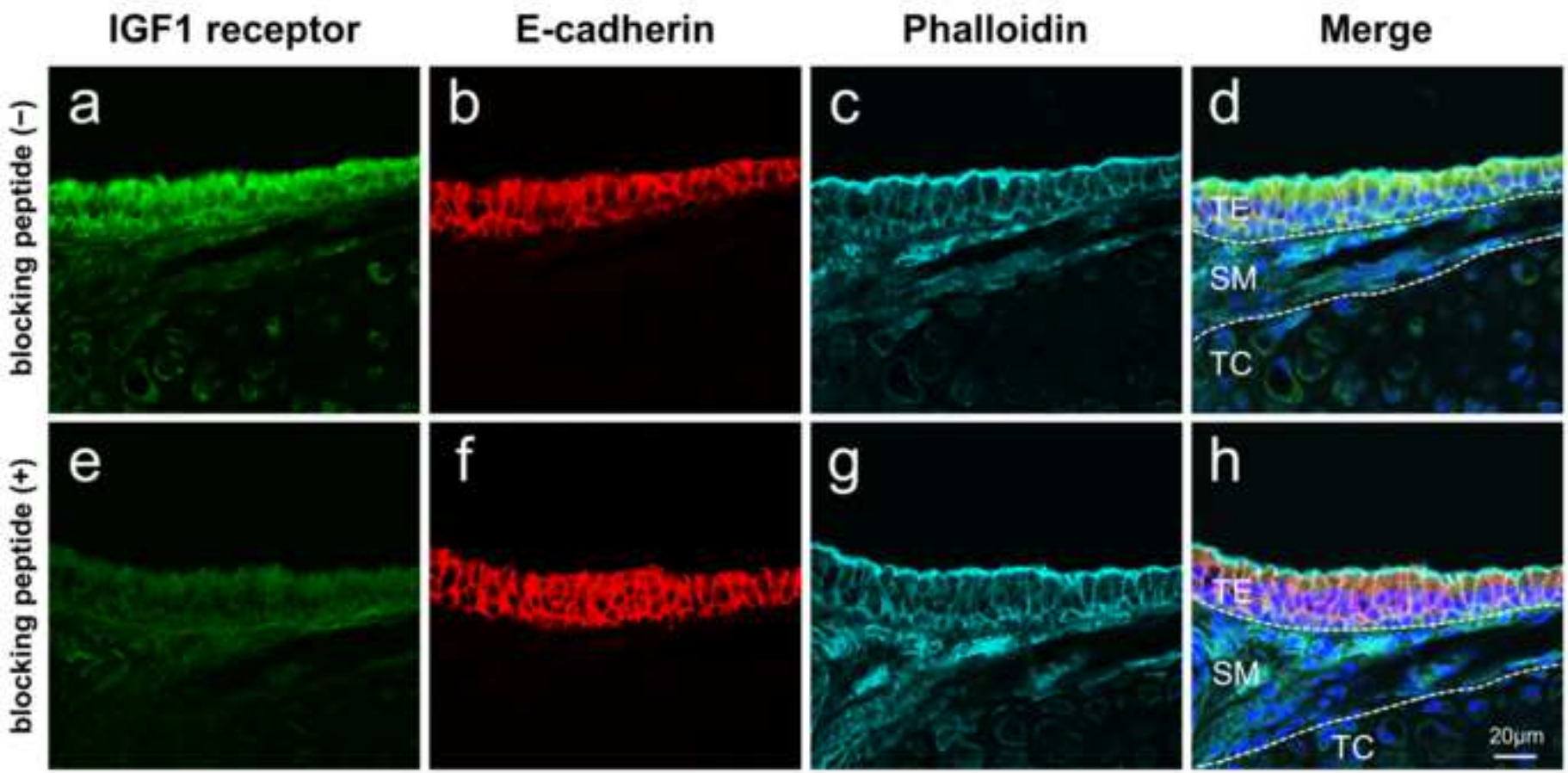
IGF1 receptor
E-cadherin
Phalloidin
Merge
blocking peptide (−)
blocking peptide (+)
a
b
c
d
e
f
g
h
TE
SM
TC
TE
SM
TC
20μm

Figure4

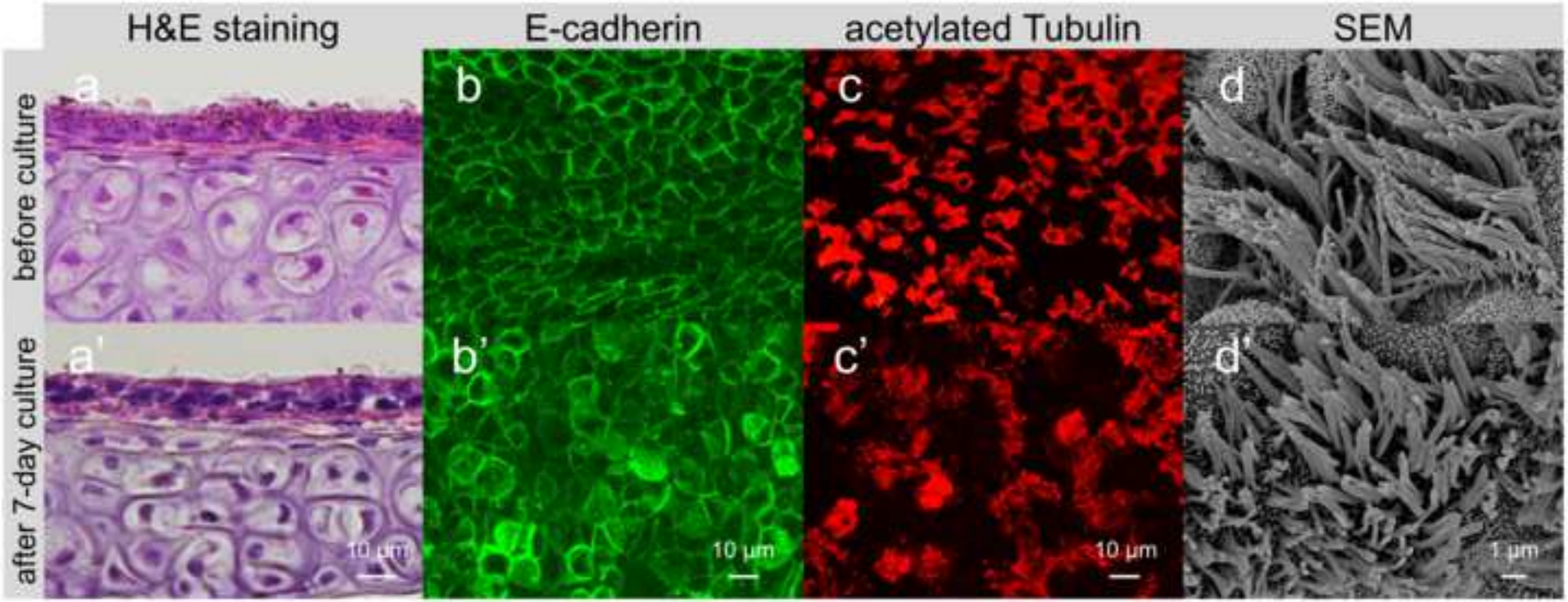
H&E staining
E-cadherin
acetylated Tubulin
SEM
before culture
after 7-day culture
a
a'
b
b'
c
c'
d
d'
10 μm
10 μm
10 μm
1 μm

Figure5

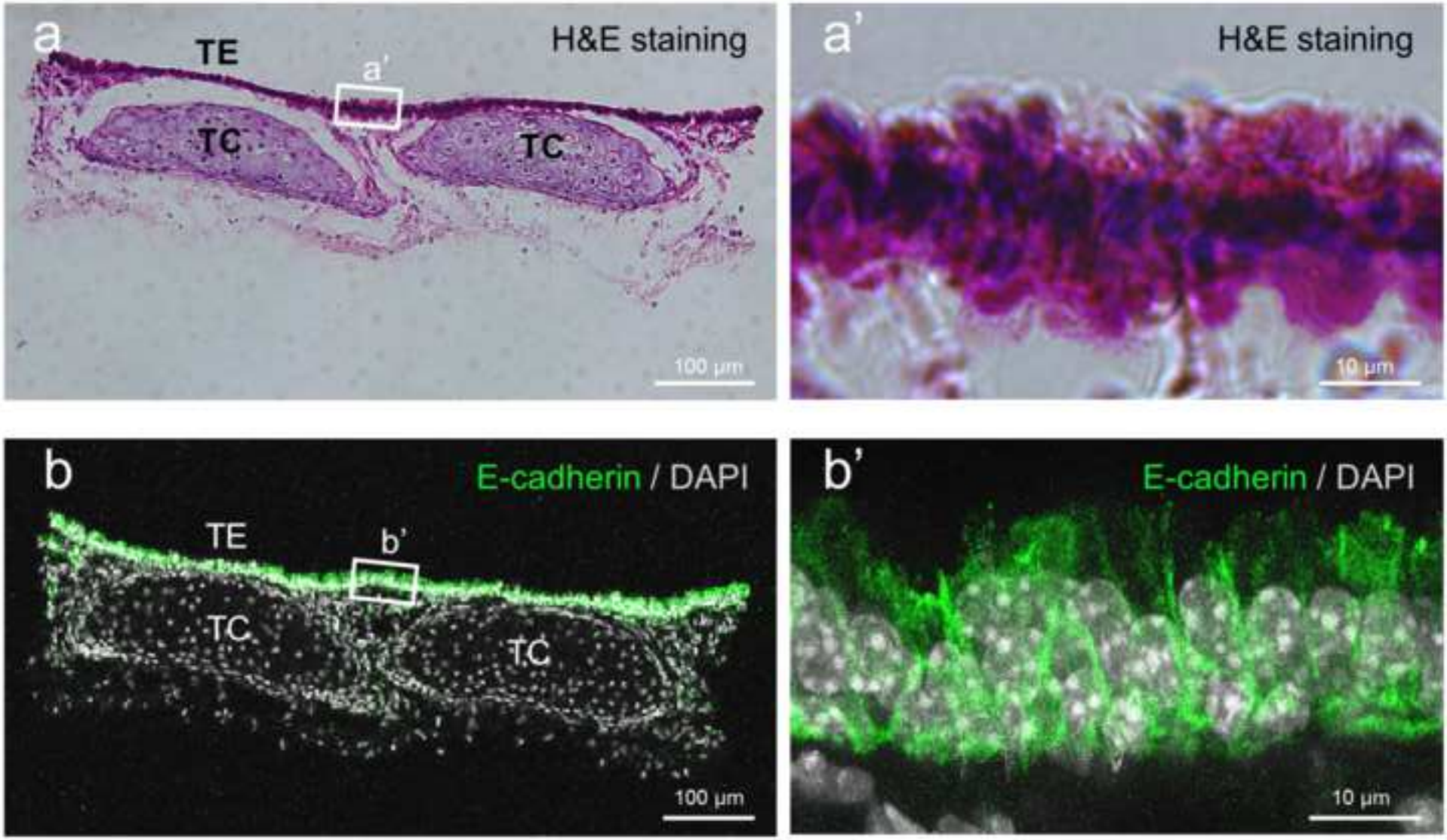
a
H&E staining
TE
a'
TC
TC
100 µm
a'
H&E staining
10 µm
b
E-cadherin / DAPI
TE
b'
TC
TC
100 µm
b'
E-cadherin / DAPI
10 µm

Figure 6

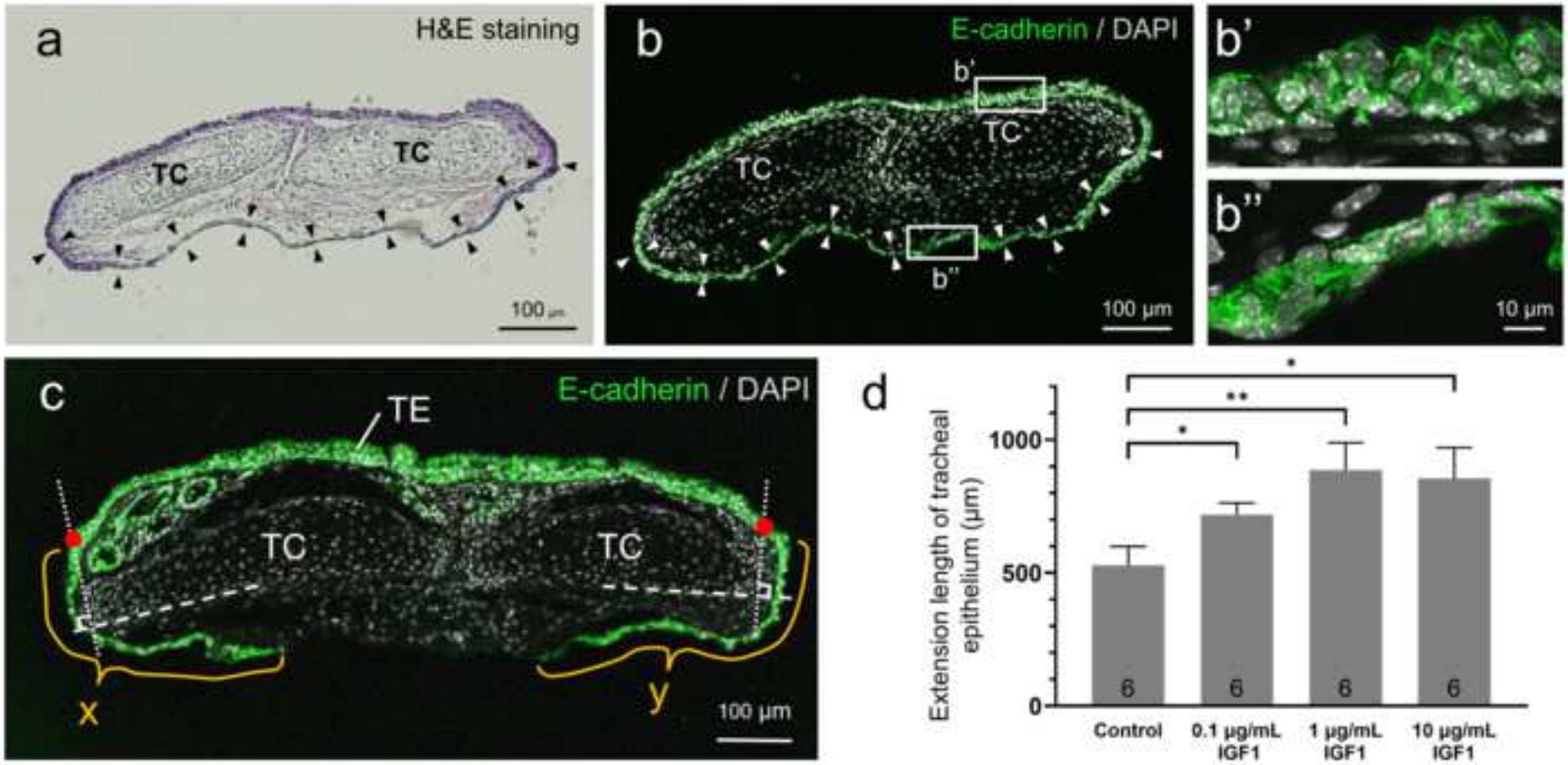
a
H&E staining
TC
TC
100 µm
b
E-cadherin / DAPI
b'
TC
TC
b''
100 µm
b'
b''
10 µm
c
E-cadherin / DAPI
TE
TC
TC
x
y
100 µm
d
Extension length of tracheal epithelium (µm)
1000
500
0
6
6
6
6
Control
0.1 µg/mL IGF1
1 µg/mL IGF1
10 µg/mL IGF1
*
**
*

Figure 7

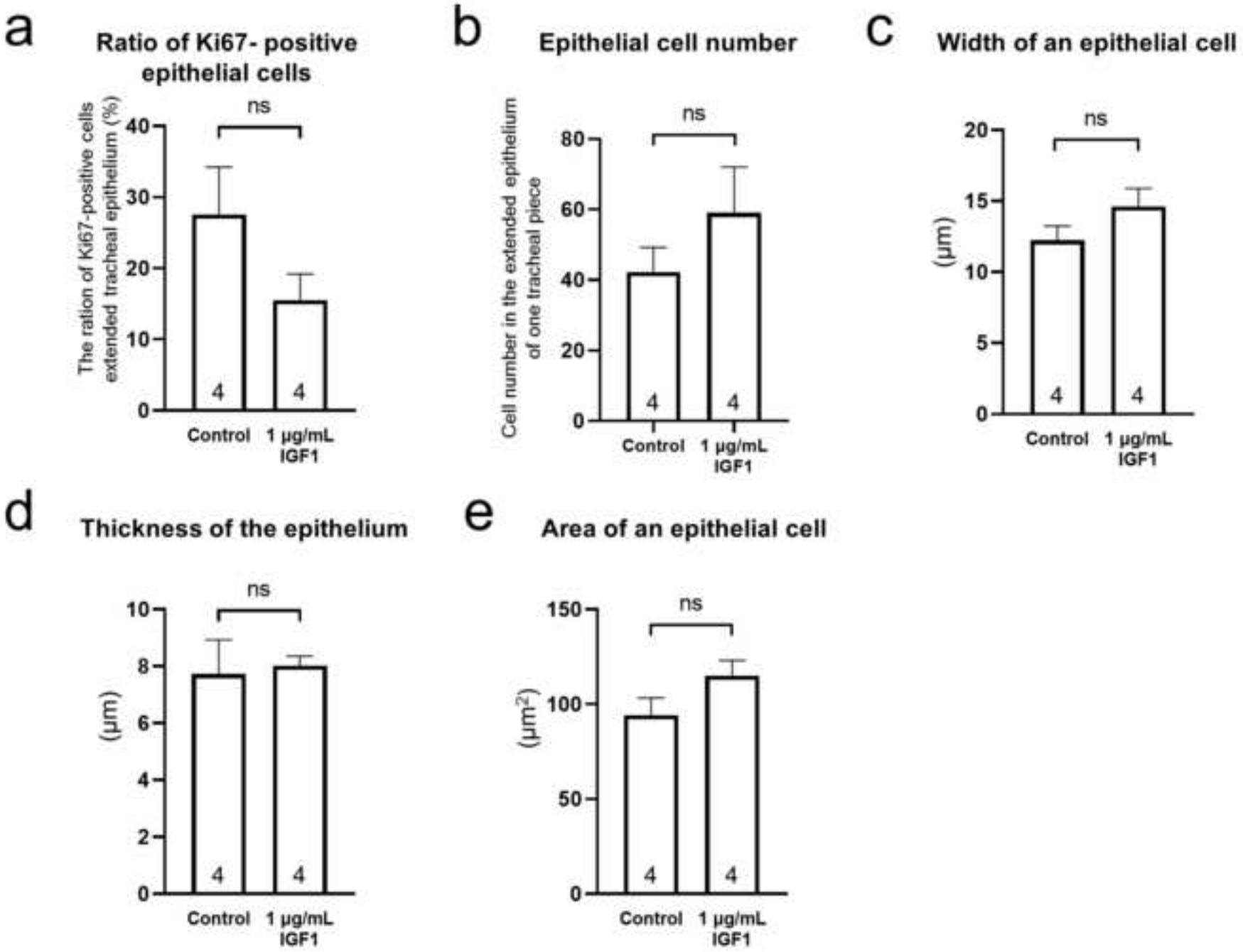
a
Ratio of Ki67- positive epithelial cells
The ration of Ki67-positive cells extended tracheal epithelium (%)
ns
40
30
20
10
0
4
4
Control
1 μg/mL IGF1
b
Epithelial cell number
Cell number in the extended epithelium of one tracheal piece
ns
80
60
40
20
0
4
4
Control
1 μg/mL IGF1
c
Width of an epithelial cell
(μm)
ns
20
15
10
5
0
4
4
Control
1 μg/mL IGF1
d
Thickness of the epithelium
(μm)
ns
10
8
6
4
2
0
4
4
Control
1 μg/mL IGF1
e
Area of an epithelial cell
(μm²)
ns
150
100
50
0
4
4
Control
1 μg/mL IGF1